



Doping-Driven Property Modulation in Thin Films Synthesized by Spray Pyrolysis

Abhilash Phulmante¹, Digvijay Gore¹, P. L. Sarwade¹, V. A. Chaudhari¹, V. D. Mote¹, S. L. Bhise², Chandrakant Londhe^{2*}

¹Thin films and materials research laboratory, Department of Physics, Dayanand Science College, Latur 413512, Maharashtra, India.

²Department of Physics Mahatma Gandhi College Ahmedpur 413515 Latur, Maharashtra, India

ABSTRACT

In this study, we designed pure NiO and CuO thin films by the spray pyrolysis method on glass substrate. The doping effect at 7% is traced by adding 'Li dopant in NiO' and 'Fe dopant in CuO' films. The confirmation of the film formation and structural modifications was observed by XRD analysis. NiO film shows cubic and CuO film has monoclinic morphology. The crystalline size is changed in both dopings. For NiO size was reduced from 14 to 9 nm. Similarly, for CuO size increment takes place from 9.6 to 10 nm.

Keywords: NiO, CuO, Spray pyrolysis, Crystalline size.

1. Introduction

"Transition metal oxides such as nickel oxide (NiO) and copper oxide (CuO) have garnered significant interest due to their versatile electrical, optical, and catalytic properties, which make them ideal for a wide range of applications including gas sensors, transparent conductive films, solar cells, and electrochromic devices [1–3]. NiO is a wide band gap p-type semiconductor with a cubic crystal structure, while CuO is a narrow band gap p-type semiconductor exhibiting a monoclinic structure [4,5]. The physical and chemical properties of these oxides can be effectively tuned through controlled doping with suitable metal ions, thereby enhancing their performance in specific applications [6,7].

Among various deposition techniques, spray pyrolysis is considered a simple, cost-effective, and scalable method for the synthesis of high-quality thin films with good uniformity and control over composition [8,9]. In this study, pure NiO and CuO thin films were synthesized using spray pyrolysis on glass substrates. The effect of 7% doping was studied by incorporating lithium (Li) into NiO and iron (Fe) into CuO thin films."

2. Experimental details

2.1 Substrate cleaning

A glass substrates are dipped in chromic trioxide for 24 hours. After that, substrates are washed under running distilled water.

2.2 Li-doped NiO Thin Films

"Li-doped NiO thin films were synthesized using the spray pyrolysis technique. A 0.1 M solution of nickel acetate tetrahydrate was used as the base precursor, and lithium acetate dihydrate was added in varying concentrations (0, 1, 3, and 5 wt%) to prepare doped samples. The mixed solution was stirred for 15 minutes and then sprayed onto glass substrates preheated to 350 °C." The spray rate was maintained at 3 ml/min with compressed air as the carrier gas. Upon heating, the precursor decomposed, forming uniform and adherent Li-doped NiO thin films.

2.3 Fe-doped CuO Thin Films

Fe-doped CuO thin films were prepared using the chemical spray pyrolysis method. Aqueous solutions of 0.1 M copper acetate monohydrate and iron nitrate nonahydrate were used as precursors. The iron dopant was introduced in concentrations of 0, 1, 3, and 5 wt% by mixing appropriate volumes of the solutions. The final mixture was stirred and sprayed onto glass substrates maintained at 350 °C. The spray resulted in the thermal decomposition of the precursors and the formation of Fe-doped CuO films with good surface uniformity and adhesion.

3. Results and discussion

3.1 Structural analysis

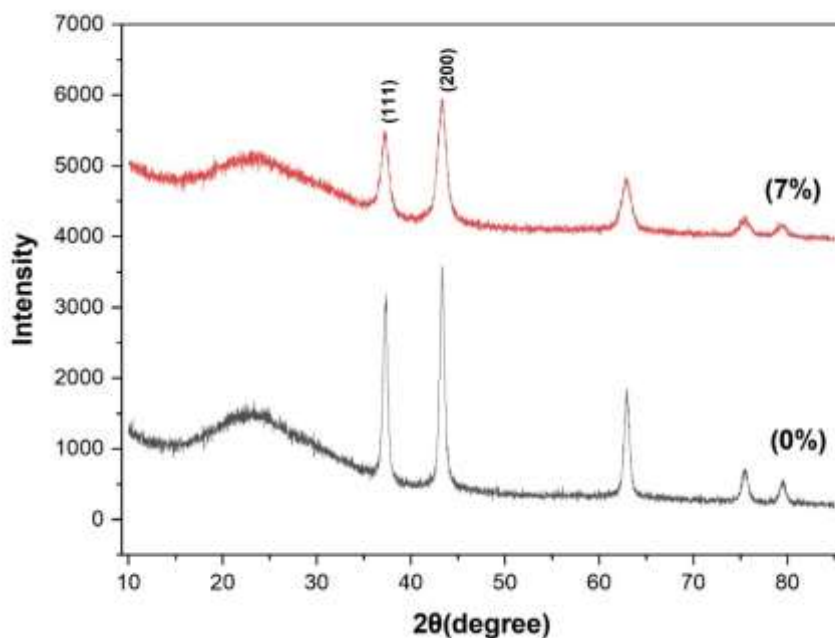


Fig2: XRD of NiO & Li doped NiO thin films.

X-ray diffraction is generally used to study structural properties of synthesised material in the form of powder or a thin film. Above Fig 2. shows the X-ray diffractogram of NiO thin film. The multiple Bragg's diffraction peaks recorded confirm the cubic phase of as deposited NiO thin film. The Bragg peaks of high intensity were recorded at Bragg's angles, $2\theta = 37.02$ and 43.91 where as additional weak peaks were located. The X-ray diffraction data of as deposited CuO thin film was in good agreement with JCPDC card 78-0643. The different planes of orientation of as deposited film at different Bragg angles were reported as (111), (200).

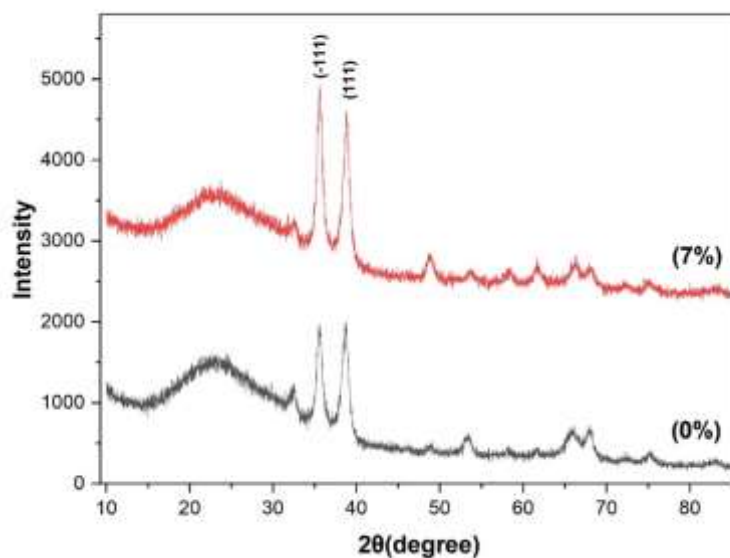


Fig3: XRD of CuO & Fe doped CuO thin films

The XRD pattern, as depicted in Fig 3, confirms the formation of the monoclinic phase of CuO. Prominent diffraction peaks were observed at 2θ values of 35.02° and 38.91° , corresponding to the characteristic reflections of monoclinic CuO. Additionally, several weak diffraction peaks were detected, indicating the monoclinic nature of the deposited film. The obtained diffraction pattern exhibited excellent agreement with the standard data (JCPDS

Card No. 80-1916), thereby validating the phase purity of the synthesized material. The major diffraction peaks were indexed to the (-111) and (111) crystallographic planes.

Grain size (D) of as deposited CuO thin film was calculated using Debye Scherrer's formula stated in equation

$$D = \frac{0.9\lambda}{\beta \cos \theta}$$

Where, (β) is the half-width of full maxima, ($k = 0.9$) is Scherrer's constant and ($\lambda = 1.54 \text{ \AA}$) is the Cu K α -radiation wavelength. The average size of a crystallite for NiO was calculated to be 14 nm. After doping, the crystallite size was reduced up to 9 nm. In the case of CuO, the size increases after 7% of Fe doping. For pure CuO it is 9.6 nm and for Fe doped CuO it is 10 nm.

4. Conclusion

In this work, pure and doped NiO and CuO thin films were successfully synthesized using the spray pyrolysis technique. X-ray diffraction analysis confirmed the formation of cubic-structured NiO and monoclinic-structured CuO thin films. The incorporation of Li and Fe dopants at 7 % induced noticeable changes in the crystallite size, reflecting modifications in the structural properties. Specifically, Li doping reduced the crystallite size of NiO, suggesting grain refinement, while Fe doping led to a slight increase in the crystallite size of CuO, indicating improved crystallinity. These findings demonstrate that doping plays a significant role in tailoring the structural characteristics of metal oxide thin films, potentially enhancing their functional performance for various technological applications

Credit authorship contribution statement

Digvijay: Central theme, Conceptualization, **V.A. Chaudhari:** literature survey,

P.L. Sarwade: Draft preparation. **Abhilash:** Methodology, Characterization analysis. **V.D.Mote:** Literature survey. **Chandrakant:** Supervision, Reviewing the manuscript

Declaration of competing interest

The authors affirm that, there are no known financial interests or personal relationships that could have appeared to influence the research work reported in this paper.

References

1. G.F. Fine et al., Metal oxide semi-conductor gas sensors in environmental monitoring. *Sensors* 10(6), 5469–5502 (2010)
2. P. Shankar, J.B.B. Rayappan, Gas sensing mechanism of metal oxides: the role of ambient atmosphere, type of semiconductor and gases-a review. *Sci. Lett. J.* 4, 126 (2015)
3. D. Li et al., Conductometric chemical sensor based on individual CuO nanowires. *Nanotechnology* 21(48), 485502 (2010)
4. Y.-B. Zhang et al., Enhanced ethanol gas-sensing properties of flower-like p-CuO/n-ZnO heterojunction nanorods. *Sens. Actuators B* 202, 500–507 (2014)
5. Y. Chen, C.L. Zhu, G. Xiao, Reduced-temperature ethanol sensing characteristics of flower-like ZnO nanorods synthesized by a sonochemical method. *Nanotechnology* 17(18), 4537–4541 (2006)
6. Z. Wang et al., CuO nanostructures supported on Cu substrate as integrated electrodes for highly reversible lithium storage. *Nanoscale* 3(4), 1618–1623 (2011)
7. Z. Li et al., Room-temperature high-performance H₂S sensor based on porous CuO nanosheets prepared by hydrothermal method. *ACS Appl. Mater. Interfaces* 8(32), 20962–20968 (2016)
8. S.J. Choi et al., Selective detection of acetone and hydrogen sulfide for the diagnosis of diabetes and halitosis using SnO₂ nanofibers functionalized with reduced graphene oxide nanosheets. *ACS Appl. Mater. Interfaces* 6(4), 2588–2597 (2014)
9. W. Jin et al., One-step synthesis and highly gas-sensing properties of hierarchical Cu-doped SnO₂ nanoflowers. *Sens. Actuators B* 213, 171–180 (2015)
10. D. Xue et al., Hydrothermal synthesis of CeO₂-SnO₂ nanoflowers for improving triethylamine gas sensing property. *Nanomaterials* 8(12), 1025 (2018)
11. J.G. Monroy, J. Gonzalez-Jimenez, J.L. Blanco, Overcoming the slow recovery of MOX gas sensors through a system modeling approach. *Sensors (Basel)* 12(10), 13664–13680 (2012)

-
12. C. Yang et al., Gas sensing properties of CuO nanorods synthesized by a microwave-assisted hydrothermal method. *Sens. Actuators B* 158(1), 299–303 (2011)
 13. H. Kim et al., H₂S gas sensing properties of bare and Pd-functionalized CuO nanorods. *Sens. Actuators B* 161(1), 594–599 (2012)
 14. Q. Zhang et al., CuO nanostructures: synthesis, characterization, growth mechanisms, fundamental properties, and applications. *Prog. Mater. Sci.* 60, 208–337 (2014)
 15. H.J. Park et al., A ppb-level formaldehyde gas sensor based on CuO nanocubes prepared using a polyol process. *Sens. Actuators B* 203, 282–288 (2014)